Chemistry & Biology, Vol. 11, 247–259, February, 2004, ©2004 Elsevier Science Ltd. All rights reserved. DOI 10.1016/j.chembiol.2004.01.015

Synthesis and Target Identification of Hymenialdisine Analogs

Yongqin Wan,[1] Wooyoung Hur,[1] Charles Y. Cho,[2] Yi Liu,[1] Francisco J. Adrian,[1] Olivier Lozach,[3] Stéphane Bach,[3] Thomas Mayer,[4] Doriano Fabbro,[4] Laurent Meijer,[3] and Nathanael S. Gray[1,*]

[1]Genomics Institute of the Novartis Research Foundation
Department of Chemistry
10675 John Jay Hopkins Drive
San Diego, California 92121

[2]The Scripps Research Institute
Department of Chemistry
10550 N. Torrey Pines Road
La Jolla, California 92037

[3]CNRS, Cell Cycle Group
Station Biologique, B.P. 74
29682 Roscoff Cedex
Bretagne
France

[4]Oncology Research
Novartis Pharma AG
CH-4002 Basel
Switzerland

Summary

Hymenialdisine (HMD) is a sponge-derived natural product kinase inhibitor with nanomolar activity against CDKs, Mek1, GSK3β, and CK1 and micromolar activity against Chk1. In order to explore the broader application of the pyrrolo[2,3-c]azepine skeleton of HMD as a general kinase inhibitory scaffold, we searched for additional protein targets using affinity chromatography in conjunction with the synthesis of diverse HMD analogs and profiled HMD against a panel of 60 recombinant enzymes. This effort has led to nanomolar to micromolar inhibitors of 11 new targets including p90RSK, KDR, c-Kit, Fes, MAPK1, PAK2, PDK1, PKCθ, PKD2, Rsk1, and SGK. The synthesis of HMD analogs has resulted in the identification of compounds with enhanced and/or dramatically altered selectivities relative to HMD (28n) and in molecules with antiproliferative activities 30-fold higher than HMD (28p).

Introduction

Protein kinases play an essential role in regulating various cellular functions including gene expression, cellular proliferation, differentiation, membrane transport, and apoptosis [1–7]. Aberrant kinase activities have been associated with several diseases including cancer, diabetes, and Alzheimer's disease [8–13]. As a consequence, considerable effort has been directed toward the development of specific and potent small molecule inhibitors of kinase function. While there are a few examples of non-ATP competitive kinase inhibitors [14, 15], the majority of kinase inhibitors target the ATP binding pocket of the enzyme. These ATP site-directed inhibitors fall into a limited number of families including quinazolines [16], pyrimidines [17–20], indolinones [21, 22], purines [23–28], imidazoles [29–31], flavonoids [32, 33], paullones [34–36], and alkaloids (for example, staurosporine and its derivatives [37–39]). To date, approximately 46 kinase inhibitors have entered clinical trials targeting kinases involved in cancer (EGFR, CDKs, Raf, PKC, PKA, KDR, Mek-1), angiogenesis (KDR), leukemia (bcr-abl, FLT3), inflammation (p38), immune disorder (JNK), and neurodegenerative disorders (JNK).

In this paper, we report the use of affinity chromatography and in vitro enzymatic profiling against a panel of 60 kinases to identify additional potential targets of the natural product Hymenialdisine (HMD **1**), as well as synthesis and biological characterization of a variety of analogs. HMD is one member of a family of tricyclic pyrrole compounds that is constructed from a brominated pyrrolo[2,3-c]azepine skeleton and a 5-membered glycocyamidine ring system. It was isolated from marine sponges including *Hymeniacidon aldis*, *Axinella verrucosa*, and *Acanthella aurantiaca* in the early 1980s based on its antiproliferative effects on cultured lymphocytic leukemia cells [40–44]. It was later shown to exhibit strong inhibitory activity against several closely related CDKs, such as CDK1/cyclin B (IC_{50} = 22 nM), CDK2/cyclin A (IC_{50} = 70 nM), CDK2/cyclin E (IC_{50} = 40 nM), and CDK5/p25 (IC_{50} = 28 nM), as well as against more distantly related kinases such as GSK3β (IC_{50} = 10 nM) and CK1 (IC_{50} = 35 nM) [45]. HMD was also isolated from the sponge *Stylissa massa* as the compound inhibiting the Raf/Mek-1/MAPK cascade and shown to be a potent inhibitor of Mek1 (IC_{50} = 6 nM) [46]. Kinetic analysis has shown that HMD acts in an ATP-competitive fashion [45], and the cocrystal structure with CDK2 revealed that HMD occupies the ATP site and makes many of the hydrogen bonding interactions seen in other CDK-inhibitor complexes [45]. Despite potent activities against these kinases, HMD is relatively selective in vitro and exhibits only moderate to weak activity against many other kinases [45–50].

The activities of HMD as a potential antiproliferative, anti-inflammatory, and antineurodegenerative agent have been investigated in several cellular models. For example, HMD in the micromolar range was shown to have antiproliferative effects against human tumor cell lines, presumably as a result of CDK and Mek inhibitory activity [46]. Using U937 cells, HMD was shown to be a micromolar inhibitor of NFκB-mediated gene transcription [51–53]. Furthermore, the hyperphosphorylation of tau, a known component of the neurofibrillary plaques characteristic of patients with Alzheimer's disease, is inhibited in vitro by HMD at 50 μM [45].

In order to identify additional potential intracellular targets of HMD, we performed affinity chromatography with immobilized HMD using brain extracts. Previously,

*Correspondence: ngray@gnf.org

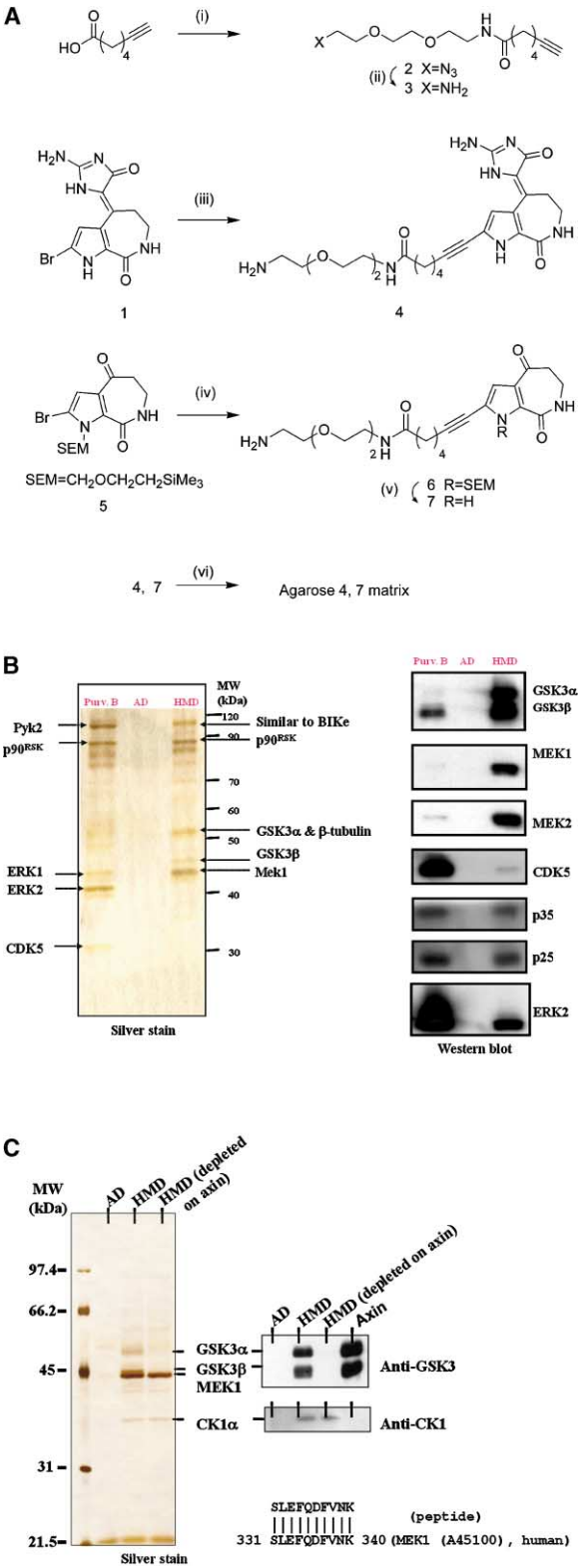

Figure 1. Preparation of Hymenialdisine and Aldisine Control Affinity Resins and Affinity Chromatography Pull-Down Experiment

(A) Synthetic scheme for Hymenialdisine (HMD) and aldisine (AD) affinity resins. (i) 6-heptynoic acid, 2-[2-(2-azido-ethoxy)-ethoxy]-ethylamine, 1,3-diisopropylcarbodiimide, CH_2Cl_2; (ii) **2**, PMe_3, THF-1% H_2O; (iii) HMD **1**, **3**, $PdCl_2(PPh_3)_2$, CuI, PPh_3, Et_2NH, DMF; (iv) 2-bromoaldisine **5**, **3**, $PdCl_2(PPh_3)_2$, CuI, PPh_3, Et_2NH, DMF; (v) a. MeOH/10% aq. HCl (1:1), b. aq. NH_3 in MeOH/H_2O (1:1); (vi) 3 mM of **4** or **7** in DMSO, 1 ml of Affi-Gel 10 Gel (Bio-Rad Laboratory), 24 hr.

(B) HMD-affinity pull-down experiment data from mouse brain extracts and intracellular target identification. Purv. B, purvalanol B resin; AD, aldisine control resin; HMD, hymenialdisine resin. Brain extracts were loaded on Purv. B, AD, or HMD matrix. Bound proteins were resolved by SDS-PAGE and visualized by silver staining and by Western blotting with anti-GSK3α/β, anti-Mek1/2, anti-CDK5, anti-p25, anti-p35, and anti-Erk2.

(C) HMD-affinity pull-down experiment data from porcine brain extracts and intracellular target identification. Brain extracts were loaded on AD or HMD matrix. Bound proteins were resolved by SDS-PAGE and visualized by silver staining and by Western blotting with anti-GSK3α/β and anti-CK. In order to purify Mek1 for microsequencing, the extracts were also depleted of GSKs using axin beads prior to chromatography with the HMD resin.

this method has yielded valuable insights into the cellular targets of two other kinase inhibitors: purvalanol B [54] and paullone [55]. To complement this approach, we also tested HMD against a panel of recombinant kinases not previously examined.

Despite the description of the total synthesis of HMD by two research groups [56–58], there have been few reported modifications to the core structure [59, 60]. The second part of this paper describes the synthesis and the structure-activity relationship (SAR) of new HMD analogs with altered kinase selectivity profiles. Of particular interest are selected analogs that retain activity against CDKs or GSK3β, which are comparable to that of the parent compound but have enhanced selectivity. The cellular activities of these compounds have also been investigated, and selected analogs showed up to 30-fold improvement over HMD.

Results and Discussion

Identifying Additional Substrates of HMD

Affinity Chromatography

The crystal structure of CDK2 complexed with HMD revealed that HMD binds in the ATP binding pocket with its bromine pointing toward the outside of the pocket [45]. Based on this observation, we reasoned that addition of a linker moiety at the 2-position of the pyrrole ring might enable us to immobilize the compound without destroying its kinase inhibitory activity. We first synthesized HMD **1** and SEM (2-(trimethylsilyl)ethoxymethyl) protected 2-bromoaldisine **5** [56]. 2-bromoaldisine, an analog lacking the 5-membered glycocyamidine that is crucial for potent kinase inhibitory activity, was used as a negative control for the experiment. A palladium-catalyzed reaction using $Pd(PPh_3)_2Cl_2$ [61] allowed the coupling of 2-bromopyrrolo compounds to an amino-PEG linker containing a terminal alkyne. After removing the SEM group, compounds **4** and **7** were immobilized to an N-hydroxysuccinimide ester-activated agarose matrix through amide bond formation (Figure 1A).

In order to identify HMD-interacting proteins present in neuronal cells, mouse brain extracts were incubated with the HMD or aldisine (AD) control matrix. After washing the matrices to remove unbound/weakly bound pro-

teins, bound proteins were eluted and separated by SDS-PAGE (Figure 1B). Prominent bands were excised, proteolytically digested, and then subjected to MALDI mass spectrometry. This resulted in the identification of six proteins: three kinases known to be potently inhibited by HMD (GSK3α/β and Mek1), two kinases that have not been previously known to be targets of HMD (p90RSK and an unknown kinase), and β-tubulin. The unknown protein may be an isoform of BIKe (BMP2-inducible kinase) that was recently identified from a prechondroblastic cell line [62].

The ability of the affinity resin to allow identification of some known targets as well as to identify some unknown ones demonstrates the utility of this approach. Since p90RSK was identified as a new target of HMD, we then measured the IC_{50}s of HMD and linker-HMD against this enzyme. The values were found to be 0.40 and 5.6 μM, respectively. Intriguingly, as observed with immobilized paullones [55], CDK5/p25 was absent from the affinity resin, despite its presence in the brain extract and its purification on immobilized purvalanol [54]. This may be due to some steric hindrance provided by the presence of the linker, as suggested by the lower sensitivity of CDK5 to linker-HMD. Although the linker-modified purvalanol B derivative is equipotent against CDK5/p25 when compared to purvalanol B (purvalanol B IC_{50} = 2 nM versus linker-purvalanol B IC_{50} = 5 nM), the linker modification of HMD led to 10-fold decrease in potency against CDK/p25 (HMD IC_{50} = 40 nM versus linker-HMD IC_{50} = 400 nM). In addition, the other targets (GSK-3, MEK1, and CK1) may be much more abundant and directly competing with low amounts of CDK5 for binding to the ligand. Finally, it is possible that native CDK5, in contrast to recombinant CDK5, is associated with other proteins that prohibit interaction with HMD.

To confirm the proteins identified by mass spectrometry, Western blot analysis using antibodies specific to Mek1, Mek2, GSK3α, GSK3β, and CDK5/p25 was performed after affinity chromatography on purvalanol B, HMD, and AD resin. The HMD resin specifically bound Mek1, Mek2, and GSK3α/β relative to the control resin. In contrast, eluate from the purvalanol B resin stained strongly for GSK3β and CDK5/p25 but only weakly for GSK3α and Mek2.

To further validate the results obtained above, affinity chromatography with immobilized HMD was carried out using porcine brain extracts (Figure 1C). GSK3α/β and CK1 were identified by Western blot and Mek1 by microsequencing. In order to purify Mek1 further for microsequencing, the extract was depleted of GSK3s using axin beads prior to chromatography with the HMD resin [63].

Kinase Selectivity Panel

In order to identify additional potential in vitro targets, HMD was tested against a panel of 60 purified protein kinases, most of which had not been previously examined. Results expressed as a percentage of enzyme activity at 10 μM inhibitor concentration are listed in Table 1. In addition to CDKs, Chk, Erk1, GSK3β, and Mek1, known targets of HMD, we found that HMD inhibits KDR, c-Kit, Fes, MAPK1, PAK2, PDK1, PKCθ, PKD2, Rsk1, SGK, and c-Src as kinases inhibited in the micromolar range. Synthetic analogs of HMD may be discov-

Table 1. Inhibition of Enzymes by HMD at 10 μM Concentration

Kinase	% Enzyme Activity	Kinase	% Enzyme Activity	Kinase	% Enzyme Activity	Kinase	% Enzyme Activity	Kinase	% Enzyme Activity	Kinase	% Enzyme Activity
Abl(m)	25	Fes(h)	7	IKKα(h)	71	MAPKAP-K2(h)	50	PDK1(h)	4	Rsk1(h)	2
c-Abl	12	FGFR-1	18	IKKα(h)	36	MEK1 (h)	2	PKA	56	SAPK2a(h)	98
Aurora-A(h)	58	FGFR3 (h)	28	Ins-R	68	c-Met	41	PKB	47	SAPK2b(h)	93
Axl(h)	30	Flt-1	21	IR(h)	104	MKK4 (m)	23	PKBα(h)	67	SAPK3 (h)	46
Bmx(h)	76	Flt-3	16	JNK1α1(h)	48	MKK6 (h)	38	PKCα(h)-His	20	SGK(h)	9
CaMKIV(h)	28	Flt-4	36	JNK2α2(h)	29	p70S6K (h)	23	PKCθ(h)	10	c-Src	9
CDK1/cyclinB(h)	2	GSK3ß (h)	1	KDR	7	PAK2(h)	7	PKD2(h)	4	Syk(h)	51
CHK2(h)	3	HER-1	60	c-Kit	4	PDGFRα(h)	89	c-Raf(h)	82	Tek	25
CK2(h)	13	HER-2	52	Lck(h)	32	PDGFR-β	16	c-Raf-1	84	TrkB(h)	17
CSK(h)	91	IGF-1R	81	MAPK1(h)	10	PDK1	100	ROCK-II(h)	51	ZAP-70(h)	90

The results are presented as kinase activity as a percentage of that in control incubations. ATP was present at 10 μM in all assays. Assays were conducted according to the procedures in [64] and [65].

ered with enhanced potency and selectivity toward these additional kinase targets.

Synthesis of Analogs Based on HMD Scaffold

The crystal structure of CDK2 complexed with HMD has revealed multiple hydrogen bonds that are important to the interaction of HMD with the enzyme active site (Figure 4A). These include the pyrrole N1 with the carbonyl oxygen of Leu83, the carbonyl oxygen of azepine ring with the backbone amide of Leu83, the amide of the azepine ring N2 with the carbonyl oxygen of Glu81, the guanidine amino group N5 with one of the side chain oxygen atoms of Asp145 and the side chain carbonyl of Asn132, two water-mediated hydrogen bonds between the O2 of HMD with the main chain carbonyl of Asp145, and N5 of HMD with the main chain carbonyl of Gln131 [45]. Since several of these hydrogen bonds are conserved in other inhibitor-CDK complexes, they are likely to contribute to the potency of HMD against CDKs and were therefore mostly retained in our synthetic efforts. The bromine substituent, in contrast, occupies a spacious hydrophobic pocket that is more completely filled by other CDK inhibitors such as olomoucine and purvalanol [45]. In order to optimize the interactions in this region, analogs were prepared where the pyrrole ring was replaced with an indole.

Synthesis of Close Analogs of HMD

To examine the effect of various substituents on the pyrrole ring, we synthesized a series of HMD analogs as shown in Table 2. HMD (**1**), debromohymenialdisine (**8**), 3-bromohymenialdisine (**10**), and 3-bromo-2-debromohymenialdisine (**9**) were prepared according to reported procedures via hymenin (**11b**) [56–58]. As an alternative procedure, alcohol **13b**, obtained from the reduction of azepinedione **12b**, reacts with 2-aminoimidazole in methanesulfonic acid to give **11b** through an in situ generated intermediate alkene **14b** (Figure 2A). Since azepinediones can be used as common building blocks for other structural modifications, we utilized this modified scheme to prepare other HMD analogs including dichlorinated analog **15**, acetamide **16**, N-ethylated analog **17**, and 3-methyl analog **18**. Cyclization of 3-[(4,5-dibromo-1H-pyrrole-2-carbonyl)-amino]-butyric acid in PPA gave the ketone in very poor yield, presumably due to electron deficiency of the dibromopyrrole ring and steric hindrance caused by the methyl group. We therefore cyclized pyrrole-2-carboxylic acid and performed bromination after reduction of the ketone (see Supplemental Figure S1 at http://www.chembiol.com/cgi/content/full/11/2/247/DC1).

The synthesis of indole analogs is outlined in Figure 2B. The attempt to synthesize the 6-chloro substituted indole analog from acetal **20b** [58] gave indole dimer as the exclusive product. Consequently, a modified scheme was attempted. Carboxylic acids **23a-g** were cyclized in P_2O_5-methanesulfonic acid [66] to yield azepino [3,4-b]indole-1,5-diones **24a-g**. These ketones were then reduced to alcohols and reacted with aminoimidazole in methanesulfonic acid. Subsequent bromination of **26** afforded compound **27** in moderate to good yields. Hydrogenation of **27a**, **27f**, and **27g** furnished compounds **27d**, **27h**, and **27i**, respectively.

Synthesis of Hydrazone and Amide Derivatives

To further probe SAR of HMD analogs, a variety of aromatic and aliphatic groups were introduced to replace the glycocyamidine ring of HMD that can be divided into two categories: hydrazones and amides. Hydrazone derivatives **28** of the previously synthesized pyrrolo- and indolo-azepinediones were prepared by reacting ketones with aromatic hydrazines (Figure 2C). Amides **31** and **34** were prepared from carboxylic acids **30** and **33** (Figure 2D). Compound **30** was obtained from the hydrolysis of t-Boc protected ester [60]. Double bond migration occurred during ester hydrolysis under basic conditions as a result of the formation of a more stable carbanion intermediate [67, 68]. Amine building blocks chosen include various aliphatic and aromatic amines.

Biological Results and SAR

SAR on Kinase Assay

In this study, we focused on investigating the inhibitory properties of HMD analogs against purified CDK5/p25, CDK1/cyclin B, and GSK3β. The structure activity relationships (SAR) of HMD analogs were examined by measuring the in vitro inhibitory activity of each HMD analog against these three kinases. Table 2 is a summary of the IC_{50}s of close structural analogs of HMD containing the pyrrolo- or indolo-azepine skeleton and the glycocyamidine appendage.

Inhibition of CDK5/p25 by Close Structural Analogs of HMD. As shown, non-, mono-, or dihalogenation at the 2- and 3-position on the pyrrole ring has little effect on the activity of these compounds against CDK5/p25. Simple pyrrole derivatives (entry 1–5) are potent inhibitors, whereas the simple indole analog (entry 9) exhibits reduced activity. Indole substituents such as a halogen at the 7-position (entry 10–12) or a nitro/amino substituent at the 9-position (entry 16 and 17) result in derivatives that are as potent as the nonsubstituted indole analog (entry 9), whereas substitution of a nitro, amino, or methanesulfonyl group at the 7-position on the indole results in reduced potency (entry 13–15).

We next investigated the effect of substitution on the azepine ring (R_3) and glycocyamidine ring (R_4). When R_3 is a methyl group, the activity is reduced by approximately 80% for both pyrrole and indole derivatives (entry 6 versus 2 and entry 18 versus 12). This phenomenon suggests that the hydrophobic pocket adjacent to methylenes of the azepine ring is quite shallow. Alkylation or acylation of the glycocyamidine ring leads to a dramatic decrease in activity, presumably as a result of steric hindrance and loss of hydrogen bonds (entry 7, 8, and 19).

Inhibition of CDK1/cyclin B by Close Structural Analogs of HMD. HMD appears to be the most potent inhibitor of CDK1/cyclin B among its close structural analogs (entry 1 versus 2–5). The inhibitory activity of these analogs against CDK1/cyclin B appears to be more susceptible to the halogen substitution pattern on the pyrrole ring than that against CDK5/p25. In particular, introducing a bromine at the 3-position on pyrrole (entry 4) has the most negative impact on the CDK1/cyclin B activity. For indole analogs, fluorine, but not chlorine or bromine, substitution at the 7-position increases the potency (entry 10, 11, 12 versus 9).

Table 2. Close Analogs of HMD and Their Biological Activity against CDK5/p25, CDK1/cyclin B, and GSK3β

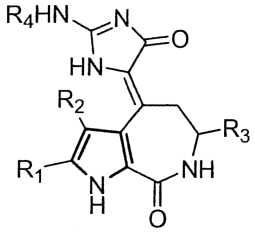

Entry	Compound Number	R_1	R_2	R_3	R_4	IC_{50}/nM CDK5/p25	CDK1/cyclin B	GSK3β
1	**1**	Br	H	H	H	37	70	73
2	**10**	Br	Br	H	H	56	530	51
3	**8**	H	H	H	H	112	250	111
4	**9**	H	Br	H	H	79	1500	90
5	**15**	Cl	Cl	H	H	62	220	47
6	**18**	Br	Br	Me	H	251	500	268
7	**16**	Br	Br	H	Ac	533	1500	363
8	**17**	Br	Br	H	Et	9120	>10000	1388

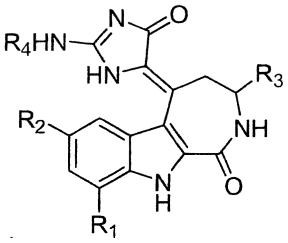

Entry	Compound Number	R_1	R_2	R_3	R_4	IC_{50}/nM CDK5/p25	CDK1/cyclin B	GSK3β
9	**27d**	H	H	H	H	177	800	64
10	**27c**	H	F	H	H	177	550	52
11	**27b**	H	Cl	H	H	191	2300	51
12	**27a**	H	Br	H	H	213	1000	47
13	**27e**	H	SO_2Me	H	H	1240	890	120
14	**27f**	H	NO_2	H	H	713	3200	710
15	**27h**	H	NH_2	H	H	681	1600	400
16	**27g**	NO_2	H	H	H	109	1200	48
17	**27i**	NH_2	H	H	H	187	1600	163
18	**27j**	H	Br	Me	H	1010	500	175
19	**27k**	H	Br	H	Ac	5110	≥10	2700

IC_{50}s were determined by two separate tests and reported as mean values. Assays were conducted at 1.5 μM ATP for CDK5/p25 and GSK3β (for SPA procedure, see Experimental Procedures) and 15 μM for CDK1/cyclin B [45].

Inhibition of GSK3β by Close Structural Analogs of HMD. When the inhibitory activity of the analogs against GSK3β was examined, we found that most of the HMD analogs are potent inhibitors. Indole derivatives generally exhibit similar activity compared to pyrrole derivatives. The substitution pattern on the indole ring has little effect on potency against GSK3β; however, alkylation or acylation of the glycocyamidine amide reduces activity (entry 7, 8 versus 2 and entry 19 versus 12).

Based on the above observations on the inhibitory properties of HMD analogs, it can be concluded that the R_3 and R_4 substituents are more influential with respect to binding activity than are R_1 and R_2. Although we believe that all these HMD analogs exhibit similar binding orientations in the ATP binding site of all three enzymes, cocrystal structures with each kinase will be needed to rationalize selectivity trends. The slightly different kinase selectivity profile among these compounds indicates the opportunity to achieve different selectivities relative to HMD. For example, the 7-bromoindole analog (entry 12) showed 10-fold improvement of selectivity between GSK3β and CDKs compared to HMD (entry 1).

Inhibition of CDK5/p25 and GSK3β by Hydrazones and Amides of HMD Analogs. In order to replace glycocyamidine ring of HMD, a variety of aryl hydrazones and amides were introduced in the context of a dibromopyrroloazepinone skeleton. Hydrazone derivatives exhibit large decreases in inhibitory activity toward CDK5/p25 and GSK3β (Figure 3, row 1). This is not surprising, as the glycocyamidine ring of HMD is known to contribute multiple hydrogen bonds to the kinase in the ATP binding pocket [45]. Previous results reported in the literature on the inhibition of CDKs, GSK3β, and CK1 by HMD-

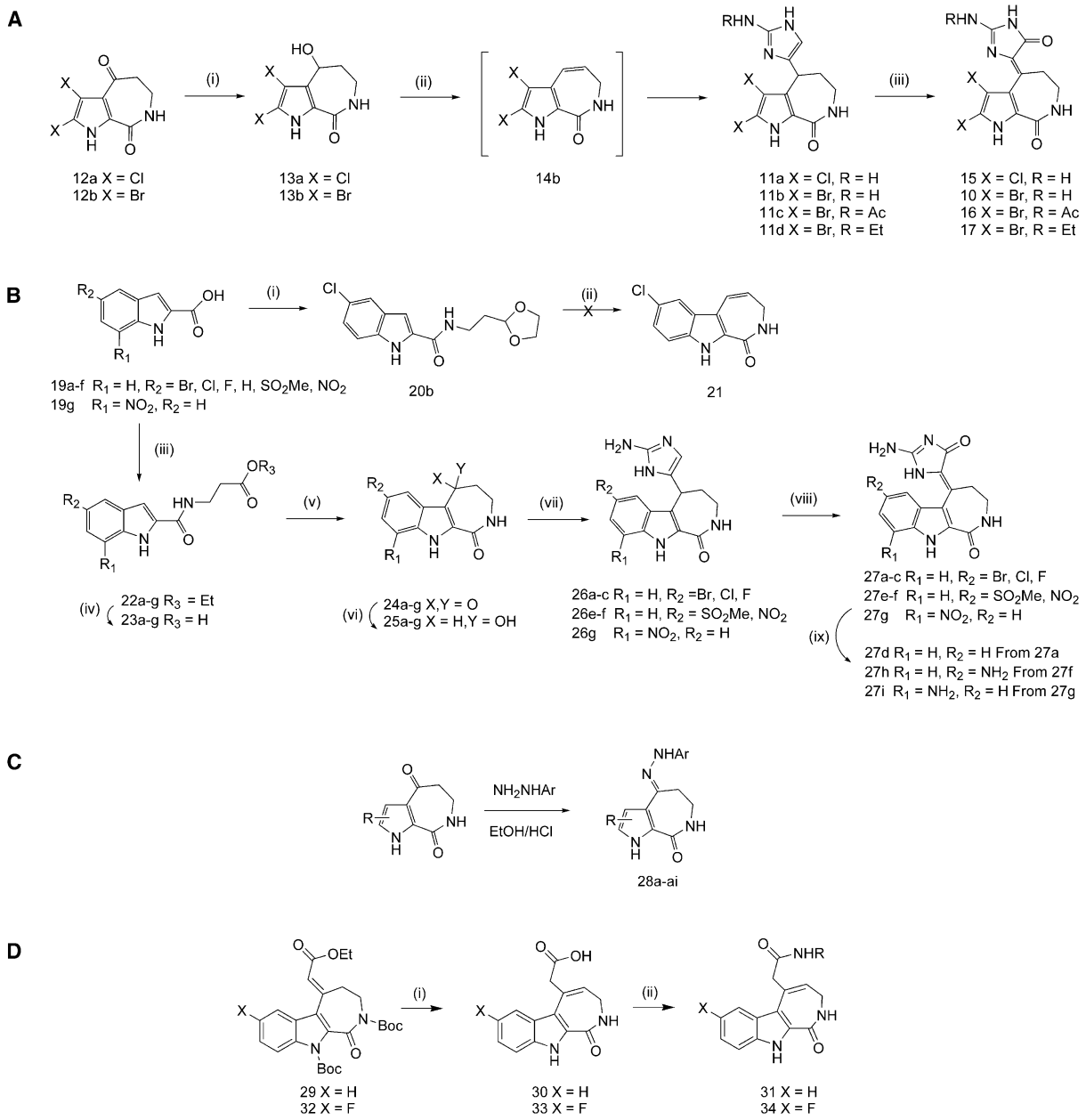

Figure 2. Synthetic Schemes for Close Analogs of HMD and Analogs Bearing Replacements to the Glycocyamidine Ring of HMD

(A) Synthetic scheme for pyrrole analogs of HMD. (i) $NaBH_4$, EtOH/DMF; (ii) 2-aminoimidazole or substituted 2-aminoimidazole, CH_3SO_3H; (iii) Br_2, NaOAc/HOAc.

(B) Synthetic scheme for indole analogs of HMD. (i) 2-(2-aminoethyl)-1,3-dioxolane, DIC, HOBt, DIEA, CH_2Cl_2; (ii) CH_3SO_3H; (iii) DIC, DIEA, HOBt, β-alanine ethyl ester; (iv) KOH; (v) P_2O_5, CH_3SO_3H; (vi) $NaBH_4$, EtOH/DMF; (vii) 2-aminoimidazole, CH_3SO_3H; (viii) Br_2, NaOAc/HOAc; (ix) H_2, 10% Pd/C or $SnCl_2$.

(C) Hydrazone derivatives.

(D) Amide derivatives. (i) a. LiOH, MeOH/H_2O; b. H^+; (ii) HATU, NH_2R, DMF.

related compounds isolated from marine sponges and few synthetically modified HMD analogs have also shown that slight structural modification of HMD has led to a dramatic drop in activity [45]. Nonetheless, hydrazones with 2-pyridyl, 3-pyridyl, or 4-sulfonamidophenyl groups exhibit CDK5/p25 IC_{50}s in the 10 μM range (compound **28c**, **28l**, **28m**). We subsequently fixed the hydrazone moiety and explored the diversity of different pyrrolo- or indolo-azepinones (Figure 3, row 2). Indole analogs show at least a 10-fold improvement in activity compared to their pyrrole counterparts. In addition, introducing a halogen at the 7-position of the indole significantly enhances the potency of derivatives against CDK5/p25 and GSK3β (compound **28t**). We prepared additional hydrazone derivatives in the context of a 5-chloro or fluoro indoloazepinone skeleton (Figure 3,

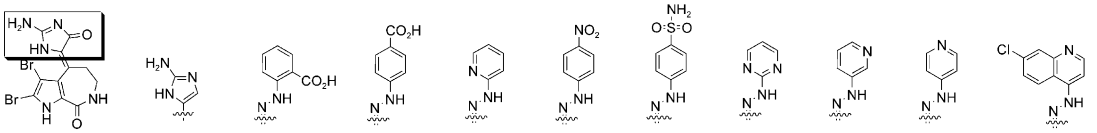

	10	11b	28a	28b	28c	28d	28e	28k	28l	28m	28j
CDK5/p25	0.056	8.15	>100	82.4	10.4	3.80	12.6	1.88	3.42	12.1	22.5
GSK3β	0.051	8.86	7.41	>33	4.28	16.6	11.6	5.97	22.3	29.7	4.66
CDK1/cyclin B	0.53	>10	ND	ND	ND	ND	ND	ND	ND	ND	ND

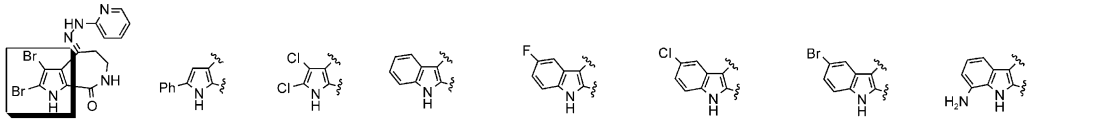

	28c	**28q**	28s	28f	28t	28g	28h	28i
CDK5/p25	10.4	23.2	6.91	0.757	0.081	0.125	0.437	22.5
GSK3β	4.28	9.13	6.99	2.62	0.171	0.399	0.741	5.95
CDK1/cyclin B	ND	ND	ND	ND	1.3	1.0	ND	ND

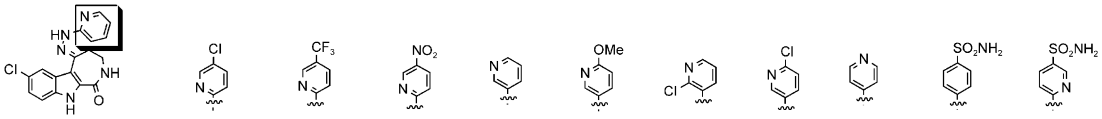

	28g	28ab	28ag	28ah	28p	28y	28aa	28ai	28o	28n	28ad
CDK5/p25	0.125	0.179	0.869	0.118	0.032	5.31	0.050	0.050	0.433	0.059	0.081
GSK3β	0.399	1.40	2.30	0.984	0.790	2.01	0.147	1.43	4.61	1.81	1.02
CDK1/cyclinB	1.0	ND	ND	ND	1.0	ND	ND	ND	ND	1.0	ND

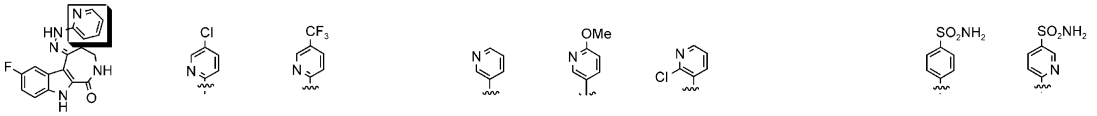

	28t	28ac	28af	28w	28x	28z	28v	28ae
CDK5/p25	0.081	0.075	0.437	0.012	2.93	0.012	0.063	0.177
GSK3β	0.171	0.613	2.24	0.557	9.59	0.088	3.45	1.99
CDK1/cyclinB	1.3	ND	ND	ND	ND	0.40	1.3	2.0

Figure 3. HMD Aanalogs with the Replacement of the Glycocyamidine Ring and Their IC_{50}s in μM against CDK5/p25, GSK3β, and CDK1/cyclin B

Assays were conducted at 1.5 μM ATP for CDK5/p25 and GSK3β (for SPA procedure, see Experimental Procedures) and 15 μM for CDK1/cyclinB [45]. Dibromopyrrolo derivatives (row 1); variations to the dibromopyrrole of the 2-pyridylhydrazones (row 2); and hydrazone variations to 5-chloro and fluoro azepinone skeletons (rows 3 and 4) (ND: not determined).

rows 3 and 4) and observed optimal CDK5/p25 inhibitory activity for 7-fluoro indole analogs with pyridyl or 4-sulfonamidophenyl hydrazone substituents (compound **28t**, **28w**, and **28v**). Pyridin-3-yl-hydrazine derivatives are more potent than the corresponding pyridin-2-yl-hydrazine and pyridin-4-yl-hydrazine ones (compound **28p** versus **28g** and **28o**). Compound **28w** and **28z** even exhibit lower IC_{50} values against CDK5/p25 than HMD. The activity of hydrazone analogs against CDK5/p25 demonstrates that the glycocyamidine ring can be replaced with other heterocycles. Attempts to create hydrazones possessing both the pyridyl and sulfonamide functionality result in no further improvement in enzyme inhibition, indicating that the interactions introduced by this functionality could not be exploited synergistically.

Most of the hydrazones obtained show much reduced potency against GSK3β compared to the close structural analogs of HMD. This result demonstrates that a favorable selectivity toward CDK5/p25 against GSK3β can be achieved. For example, hydrazone **28w** is 3-fold more potent than HMD against CDK5/p25 (IC_{50} 12 nM) but eight times less potent against GSK3β (IC_{50} 557 nM) relative to HMD. As another example, hydrazone **28v**, with 4-sulfonamidophenyl group, has an IC_{50} value twice that of HMD against CDK5/p25, but 50 times that of HMD against GSK3β.

Kinase Selectivity of HMD and Selected Analogs

To investigate how these scaffold modifications alter the specificity against a broader range of kinases, six compounds including HMD were tested against 20 different kinases at a concentration of 10 μM (Table 3). All six compounds exhibited potent activity against CDK1, and most also inhibit c-src, with the exception of sulfonamide **28n**. In general, most analogs are more selective than HMD, while the in vitro inhibitory profile of the 7-fluoroindole analog **27c** is the closest to HMD. Sulfonamide **28n** is the most selective compound among the six tested, with >95% inhibition of CDK1 and <45% inhibition of the rest of the kinases. Compounds containing amide replacement of the glycocyamidine ring (**31** and **34**) demonstrated very weak activities against CDK5/p25 and GSK3β. Potential targets of this series are still under investigation.

Docking Results

To study in detail the essential binding interaction of HMD analogs with CDK5, we performed docking studies of the inhibitors using GOLD v2.0 [69]. The CDK5 structure used for docking studies was taken from the crystal

Table 3. 20 Enzyme Inhibition Pattern for HMD and Selected Analogs: Percent Remaining Enzyme Activity at 10 μM Inhibitor Concentration

	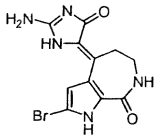	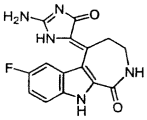	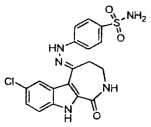	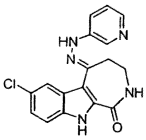	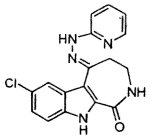	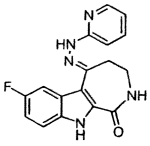
	1	27c	28n	28p	28g	28t
c-Abl	12	36	62	40	9	14
HER-1	60	81	96	64	60	69
HER-2	52	53	76	44	57	74
KDR	7	30	84	73	52	65
Flt-3	16	37	57	41	28	25
IGF-1R	81	81	70	44	18	24
c-Raf-1	84	77	74	36	53	54
PDGFR-β	16	35	79	3	32	42
Flt-4	36	56	74	78	33	33
c-Kit	4	14	67	53	21	31
Flt-1	21	49	69	72	15	21
Tek	25	61	73	30	27	19
PKA	56	61	73	76	69	62
c-src	9	11	56	22	8	10
CDK1	1	1	5	3	12	2
PKB	47	52	60	49	50	52
PDK1	100	100	100	81	89	100
Ins-R	68	81	73	52	38	46
FGFR-1	18	11	74	70	71	82
c-Met	41	26	93	43	49	88

The results are presented as kinase activity as a percentage of that in control incubations. ATP was present at 10 μM in all assays. Assays were conducted according to the procedures in [64] and [65].

structure of CDK5 in complex with p25 (PDB code 1H4L) [70]. Water and p25 were extracted from the cocomplex structure and hydrogen atoms were added to the CDK5 protein. There are four residues missing in the glycine-rich loop of CDK5 structure. Since these four residues are not important to the binding of HMD, they were not included in the docking. All atom types and charges were assigned in GOLD, and all docking parameters were taken from the standard default settings. Although the CDK2 in the CDK2-HMD complex is in an inactive conformation while CDK5 in the CDK5-p25 complex is in an active conformation, the binding pockets of HMD in CDK2 and CDK5 are structurally very similar. After superposition of 17 residues in the ATP binding pocket within 5 Å of HMD, the rmsd of C_α atoms from CDK2 and CDK5 is only 0.6 Å. We compared the model of HMD bound to active CDK5 with the crystal structure of inactive CDK2 in complex with HMD and found the interaction of HMD with protein in both structures were very similar. Experimentally, crystal structures of indirubin bound to active and inactive CDK2 also showed that a kinase inhibitor bound to active and inactive CDK2 with a similar binding mode [71].

We noticed that for the close structural analogs of HMD (Table 2), indole derivatives **27** exhibit reduced CDK5 versus GSK3β activity relative to the corresponding pyrrole analogs. One possible explanation for this differing kinase inhibitory profile of pyrrole and indole compounds is the steric interaction between the 4-H of the indole ring and the glycocyamidine amide. While the tricyclic ring system of HMD appears to be coplanar when HMD is bound to CDK2 [45], the steric repulsion prevents the glycocyamidine-indole analogs from achieving the perfect geometry for binding to CDK2 (see Supplemental Figure S2 at http://www.chembiol.com/cgi/content/full/11/2/247/DC1).

In addition to the three commonly observed hydrogen bonds between the pyrrolo- or indolo-azepinones and the backbone Glu81 and Cys83 (Leu83 in the case of CDK2-HMD complex) of the enzyme, the modeling of hydrazone analogs **28v**, **28t**, and **28w** suggested possible hydrogen bonds between the heterocyclic ring appendage and the enzyme (Figures 4C–4E). HMD may form a hydrogen bond between the amino group of the glycocyamidine and the side chain of Asp144, as well as a water-mediated hydrogen bond between the amino group of the glycocyamidine and the main chain amide of Gln130. The pyridyl groups of **28t** and **28w** may form electrostatic interactions with the Asp144 carboxylate. In addition, Gln130 is within 5 Å of the hydrazone proton, making possible a water-mediated hydrogen bond. In order to fit into the ATP pocket, sulfonamide **28v** may adopt a different geometry of the hydrazone double bond from pyridyl compounds **28t** and **28w**. It may be capable of forming a hydrogen bond between the sulfonamide and the Asp144 side chain, as well as a hydrogen bond between the oxygen of the $-SO_2-$ and the Tyr11 NH. The different hydrogen bonding mode could be responsible for compound **28v**'s different kinase selectivity profile. Docking **28t** or **28w** with a different double bond geometry leads to less favorable inhibitor-kinase interactions. As the orientation of heterocyclic appendage of the hydrazones is quite different from that of HMD, we propose that the 10-fold improved potency

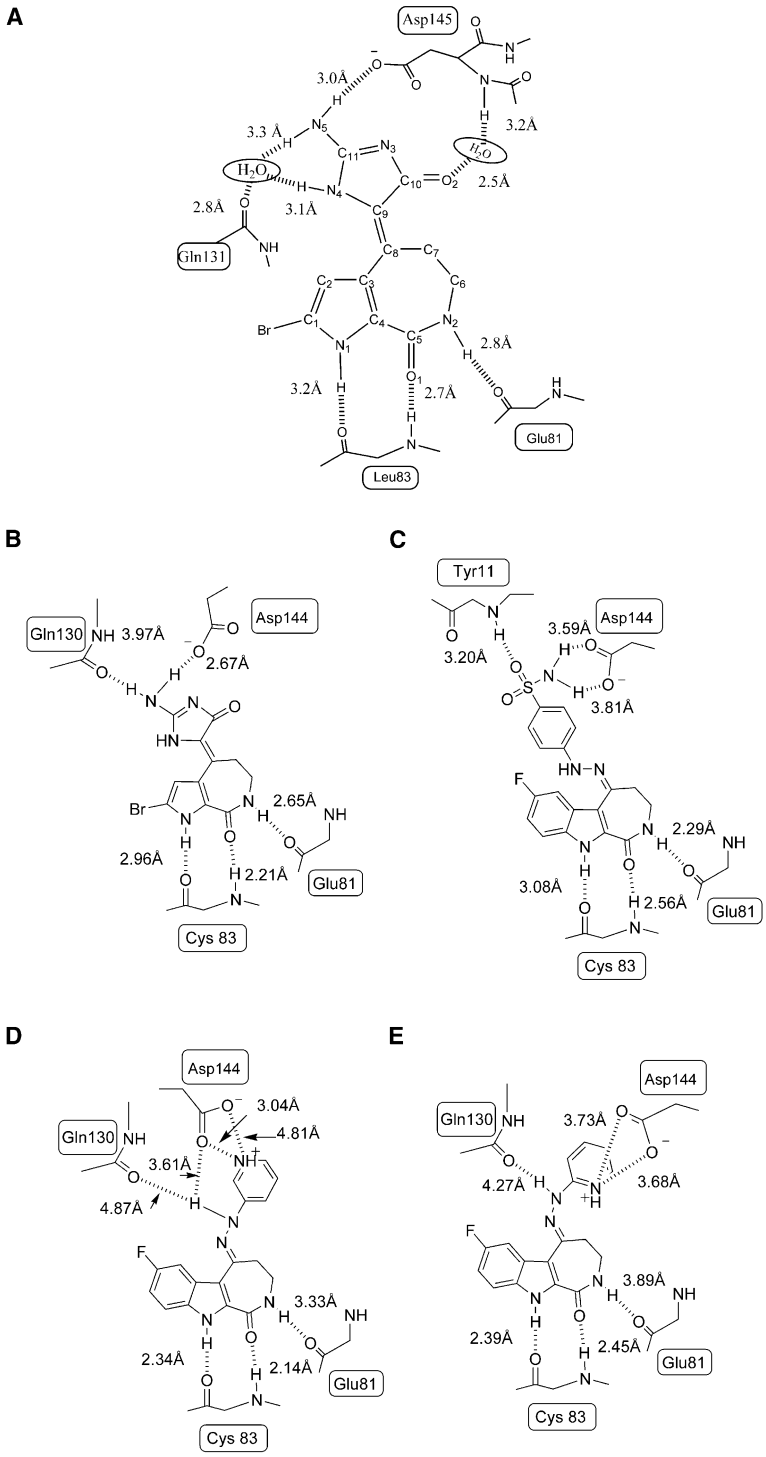

Figure 4. Illustration of Possible Interactions between HMD or Its Analogs with CDK2 or CDK5/p25

Hydrogen bonds and electrostatic interactions are indicated by broken lines.
(A) Cartoon illustration of key hydrogen bonds in HMD and CDK2 complex, reproduced according to [45].
(B) HMD and CDK5/p25.
(C) Hydrazone **28v** and CDK5/p25.
(D) Hydrazone **28w** and CDK5/p25.
(E) Hydrazone **28t** and CDK5/p25.

against CDK5/p25 and GSK3β of the hydrazone indoles (e.g., compound **28w**, Figure 3) versus the glycocyamidine indoles (e.g., **27c**, Table 2) results from a more optimal orientation of the hydrazone heterocycle relative to the indole core to relieve strain from the indole 4-H position.

Cellular Effects and Cell Cycle Studies

To assess the efficacy of these compounds as CDK inhibitors in a cellular context, we treated 786-O renal adenocarcinoma cells with selected compounds and characterized cell proliferation and DNA content redistributions in the population using fluorescence microscopy. The majority of unsynchronized 786-O cells growing in serum are in G1 phase (53.1% ± 1.6%), with 16.1% ± 0.9% and 30.8% ± 1.6% in S and G2/M phases, respectively (see Supplemental Figure S3 and Table S2 at http://www.chembiol.com/cgi/content/full/11/2/247/DC1). Inhibition of CDK1/cyclin activity results in G2/M

arrest [3]. Although HMD is an effective inhibitor of CDK1/cyclin B activity in vitro (IC_{50} = 70 nM), its cell cycle progression inhibitory effect in 786-O cells is modest. The lowest concentration of HMD tested that results in significant (>40%) G2/M arrest is 100 μM (Supplemental Table S2). While this discrepancy between enzymatic and cellular activity is large, it is generally consistent with an earlier study that shows HMD inhibition of GSK3 activity at 50 μM in cells [45].

HMD analogs that were most similar to HMD in structure similarly showed limited cellular activity. Compounds **10**, **15**, **27a**, **27b**, **27c**, **27d**, and **27g** had no effect on the percentage of cells in G2/M phase up to 30 μM and no growth inhibition phenotype up to 15 μM. A key structural feature that these compounds share with HMD is the highly polar glycocyamidine ring, which may limit the compounds' cell permeability. Other compounds tested that were inactive included hydrazones **28c**, **28e**, **28l**, **28n**, and **28v**. These compounds either had low CDK inhibitory activity (**28c** and **28l**) or sulfonamide groups that seemed to inhibit cellular activity (**28e**, **28n**, and **28v**).

The compounds with the highest inhibition of cell growth were indole-hydrazone analogs. Compounds **28p**, **28w**, and **28z** (Figure 3, rows 3 and 4) arrested cells in G2/M phase at concentrations as low as 3.8 μM (Supplemental Figure S3C and Table S2 at http://www.chembiol.com/cgi/content/full/11/2/247/DC1). Compounds **28t**, **28g**, and **28ai** did not alter the percentage of cells in G2/M phase but significantly inhibited cell proliferation. These compounds may have a more complex kinase inhibitory profile (inhibiting targets that result in G1 arrest in addition to CDK1/cyclin A) or act by other mechanisms that cause cell death.

Significance

Several protein kinase inhibitors have advanced to clinical trials based on the indolocarbazole nucleus of Staurosporine (PKC412, Novartis; CEP-701, Cephalon; LY-333531, Eli Lilly). The pyrrole[2,3-c]azipine scaffold of HMD also exhibits great potential for development as a therapeutically relevant kinase inhibitor scaffold. The present work facilitates this goal by demonstrating that analogs of HMD can be prepared by a variety of synthetic routes and that these compounds posses altered potencies and selectivities toward a variety of therapeutically relevant kinases.

Experimental Procedures

Preparation and Use of Affinity Reagents

Affi-Gel 10 Gel (Bio-Rad Laboratory) (1 ml bed volume) was rinsed with anhydrous DMSO (4 ml × 3) and transferred into a vial containing a solution of linker tethered compound **4** or **7** in DMSO (3 μM, 1 ml). The mixture was agitated at room temperature for 1 day in the presence of triethylamine (the progress of the coupling reaction was monitored by LC-MS). Upon the completion of the coupling, excess amount of ethanolamine (8 μl) was added to block any unreacted groups that remain on the resin. The resulting beads were washed with DMSO (4 ml × 3) and PBS (4 ml × 3) and stored in PBS (1 ml) at 4°C until use.

Extraction of Proteins

Mouse brains were homogenized in lysis buffer (25 mM MOPS, 15 mM EGTA, 15 mM $MgCl_2$, 2 mM DTT, 1 mM sodium orthovanadate, 1 mM NaF, 1 mM phenyl phosphate, 15 mM nitrophenyl phosphate, 60 mM β-glycerophosphate, 100 mM benzamidine, 10 μg/ml leupeptin, and 10 μg/ml aprotinin [pH 7.2]) using tissue grinders (Kontes). The resulting homogenate was centrifuged for 30 min at 20,000 × g and 4°C. The supernatant was recovered and stored at −80°C until used.

Affinity Chromatography

Affinity chromatography was performed as described in [54]. Affinity matrices (30 μl) were washed with bead buffer (50 mM Tris HCl, 5 mM EDTA, 5 mM EGTA, 5 mM NaF, 250 mM NaCl, 0.1% Nonidet P-40, 100 mM benzamidine, 10 μg/ml leupeptin, and 10 μg/ml aprotinin [pH 7.4]) twice before use and resuspended in 400 μl of bead buffer. Proteins (200 μg) in 400 μl of lysis buffer were added and incubated with rotation for 1 hr at 4°C. The resins were then washed 4 times with bead buffer and bound proteins were eluted by heating at 95°C for 3 min in the presence of 2× Lammli sample buffer. The resulting supernatants were loaded onto SDS-PAGE gels, and the separated proteins were visualized by silver staining or Western blot analysis. To identify proteins by peptide mass fingerprinting, proteins (1 mg) were loaded onto the same amount of resins and eluted proteins were stained by Coomassie brilliant blue G (Bio-Rad Laboratories).

Silver Staining

Silver staining was performed as described in [70]. Gels were fixed in 50% methanol/5% acetic acid for 20 min then washed with water for 1 hr. They were sensitized by incubating in 0.02% (w/v) $Na_2S_2O_3$ for 1 min and then washed twice with water for 1 min before being incubated in 0.1% (w/v) $AgNO_3$ for 20 min. After being washed again twice with water for 1 min, gels were developed in a solution containing 0.04% (v/v) formaldehyde and 2% (w/v) Na_2CO_3. The reaction was terminated by discarding the reagent followed by addition of 5% acetic acid in water.

Protein In-Gel Digestion

In-gel digestion was performed according to the published protocol [72] with minor modifications. Protein bands in Coomassie-stained gel were excised and rinsed with water for 15 min. They were then incubated in 100 mM NH_4HCO_3 (100 μl) for 15 min. The same volume of CH_3CN was added and incubated for 15 min. After the supernatant was removed, protein bands were shrunk by dehydration in CH_3CN. CH_3CN was removed by vacuum centrifuge and gel pieces were swollen in a digestion solution containing 50 mM NH_4HCO_3 and 12.5 ng/μl of modified porcine trypsin (Promega) in an ice-cold bath. The supernatant was removed 45 min later and replaced with 50 mM NH_4HCO_3 (15 μl) to keep gel pieces wet during the overnight enzymatic digestion at 37°C.

Sample Preparation for MS Analysis and Peptide Mass Fingerprinting Using MALDI-TOF MS

Tryptic digests were introduced to microscale purification [73], which allowed efficient concentration of peptides and cleanup of analytes. A micro purification column was prepared using a Gel-oader tip (Eppendorf, Germany), in which Poros 50 R2 (PerSeptive Biosystems) was packed and equilibrated. Samples were loaded onto the column and briefly washed with formic acid (5%, 15 μl). Peptides bound to the resin were eluted directly onto a MALDI target with 1 μl of saturated α-cyano-4-hydroxy-*trans*-cinnamic acid in acetonitrile-formic acid-water (50:5:45) solution.

The MALDI-TOF mass spectrometer (BIFLEX; Bruker Daltoniks, Germany) was operated in the reflector mode. Ion signals produced by trypsin autodigestion peptides were used as internal mass calibrants. Proteins were identified by searching against NCBI human nonredundant (nr) and SwissProt databases with the list of monoisotopic tryptic peptide masses using 200 ppm mass tolerance. Database searching was performed using a web-based search program, PROFOUND (http://prowl.rockefeller.edu/profound_bin/webProFound.exe) developed by Rockefeller University and Proteometrix [74].

Radioenzymatic RSK1 Kinase Assay

The RSK1 (p90S6K) kinase inhibitory activity of HMD and HMD-linker was evaluated following manufacturer's (Upstate) recommendations using the peptide KKLNRTLSVA as a substrate.

In Vitro Kinase Assay Using SPA Assay

SPA assay [75] was performed using SPA assay kit (Amersham Pharmacia Biotech, UK). Inhibitors dissolved in DMSO were transferred to 5 μl of enzyme in assay buffer (50 mM MOPS [pH 7.2] and 5 mM $MgCl_2$). Enzymatic reactions were initiated by adding 10 μl of solution containing 1.5 μM ATP, 1.5 μM biotinylated substrate, 0.01 μCi [γ-^{33}P]ATP (NEN Life Science) and incubated at room temperature for 1 hr in 384-well ProxiPlates (Perkin Elmer). Reactions were stopped by the addition of 10 μl PBS solution containing 50 μg of streptavidin-tagged polyvinyltoluene bead, 50 mM ATP, 5 mM EDTA, and 0.1% Triton X-100. Before counting the signals with TopCount (Packard Bioscience), the plates were spun for 3 min at 2000 rpm. For GSK3β, sequence of the peptide substrate was biotin-YRR AAVPPSPSLSRHSSPHQ(pS)EDEEE (Upstate). In CDK5/p25 assay, the peptide was biotin-aminohexanoic acid-AGAKKAVKTPKKAKKP derived from Histone H1.

Cell Cycle Studies

786-O renal adenocarcinoma cells were cultured in DMEM with 10% fetal bovine serum supplemented with glutamine and antibiotics. Cells were plated in black clear bottom 384-well microtiter plates (Greiner) and cultured for 8 hr. Compounds of interest were added to cells (<1% DMSO final concentration) and incubated for 30 hr at 37°C, with four replicate wells for each concentration. After washing with PBS, cells were fixed with 3.5% paraformaldehyde in PBS for 20 min. Nuclei were stained with 4′,6-diamidino-2-phenylindole dihydrochloride (200 ng/ml) in 0.1% TritonX-100/PBS for 1 hr. After washing with PBS, cells were imaged on an EIDAQ100 (Q3DM) automated inverted fluorescence microscope (Nikon TE300 with a Cohu video camera) with a 10×/0.5 objective (Nikon). Sixteen images were collected per well. Image analysis was performed with CytoShop software (Q3DM). After images were shade corrected and background subtracted, objects were extracted and single cells defined using geometric and total fluorescence parameters. Histograms plotting number of events versus total nuclear intensity for representative wells were used to define nuclear fluorescence boundaries for G1, S, and G2/M cells. Percentages of cells in each category were determined for all wells and replicate wells were averaged for each condition.

Supplemental Data

General synthetic methods and spectroscopic data for all compounds included in the main text, as well as cell proliferation and DNA content redistributions in the population of 786-O renal adenocarcinoma cells after treatment with selected HMD analogs, are included in the Supplemental Data at http://www.neuron.org/cgi/content/full/11/2/247/DC1.

Acknowledgments

We are grateful to Dr. Priscilla Yang and Dr. Tetsuo Uno for revising this article and providing valuable suggestions.

Received: September 19, 2003
Revised: November 18, 2003
Accepted: November 24, 2003
Published: February 20, 2004

References

1. Sridhar, R., Hanson-Painton, O., and Cooper, D.R. (2000). Protein kinase as therapeutic targets. Pharm. Res. *17*, 1345–1353.
2. García-Echeverría, C., Traxler, P., and Evans, D.B. (2000). ATP site-directed competitive and irreversible inhibitors of protein kinases. Med. Res. Rev. *20*, 28–57.
3. Sielecki, T.M., Boylan, J.F., Benfield, P.A., and Trainor, G.L. (2000). Cyclin-dependent kinase inhibitors: useful targets in cell cycle regulation. J. Med. Chem. *43*, 1–18.
4. Traxler, P., Bold, G., Buchdunger, E., Caravatti, G., Furet, P., Manley, P., O'Reilly, T., Wood, J., and Zimmermann, J. (2001). Tyrosine kinase inhibitors: from rational design to clinical trials. Med. Res. Rev. *21*, 499–512.
5. Toogood, P.L. (2001). Cyclin-dependent kinase inhibitors for treating cancer. Med. Res. Rev. *21*, 487–498.
6. Bridges, A.J. (2001). Chemical inhibitors of protein kinases. Chem. Rev. *101*, 2541–2572.
7. Scapin, G. (2001). Structural biology in drug design: selective protein kinase inhibitors. Drug Discov. Today *7*, 601–611.
8. Garrett, M.D., and Fattaey, A. (1999). CDK inhibition and cancer therapy. Curr. Opin. Gene Dev. *9*, 104–111.
9. Malumbres, M., and Barbacid, M. (2001). Milestones in cell division: to cycle or not to cycle: a critical decision in cancer. Nat. Rev. Cancer *1*, 222–231.
10. Ali, A., Hoeflich, K.P., and Woodgett, J.R. (2001). Glycogen synthase kinase-3: properties, functions, and regulation. Chem. Rev. *101*, 2527–2540.
11. Imahori, K., and Uchida, T. (1997). Physiology and pathology of tau protein kinases in relation to Alzheimer's disease. J. Biochem. (Tokyo) *121*, 179–188.
12. Mandelkow, E.-M., and Mandelkow, E. (1998). Tau in Alzheimer's disease. Trends Cell Biol. *8*, 425–427.
13. Martinez, A., Castro, A., Dorronsoro, I., and Alonso, M. (2002). Glycogen synthase kinase 3 (GSK-3) inhibitors as new promising drugs for diabetes, neurodegeneration, cancer, and inflammation. Med. Res. Rev. *22*, 373–384.
14. Profit, A.A., Lee, T.R., and Lawrence, D.S. (1999). Bivalent inhibitors of protein tyrosine kinases. J. Am. Chem. Soc. *121*, 280–283.
15. Martinez, A., Alonso, M., Castro, A., Pérez, C., and Moreno, F.J. (2002). First non-ATP competitive glycogen synthase kinase 3 (GSK-3) inhibitors: thiadiazolidinones (TDZD) as potential drugs for the treatment of Alzheimer's disease. J. Med. Chem. *45*, 1292–1299.
16. Fry, D.W., Kraker, A.J., McMichael, A., Ambroso, L.A., Nelson, J.M., Leopold, W.R., Connors, R.W., and Bridges, A.J. (1994). A specific inhibitor of the epidermal growth factor receptor tyrosine kinase. Science *265*, 1093–1095.
17. Rewcastle, G.W., Murray, D.K., Elliott, W.L., Fry, D.W., Howard, C.T., Nelson, J.M., Roberts, B.J., Vincent, P.W., Showalter, H.D., Winters, R.T., et al. (1998). Tyrosine kinase inhibitors. 14. Structure-activity relationships for methylamino-substituted derivatives of 4-[(3-bromophenyl)amino]-6-(methylamino)-pyrido[3,4-d]pyrimidine (PD 158780), a potent and specific inhibitor of the tyrosine kinase activity of receptors for the EGF family of growth factors. J. Med. Chem. *41*, 742–751.
18. Traxler, P., Bold, G., Frei, J., Lang, M., Lydon, N., Mett, H., Buchdunger, E., Meyer, T., Mueller, M., and Furet, P. (1997). Use of a pharmacophore model for the design of EGF-R tyrosine kinase inhibitors: 4-(phenylamino)pyrazolo[3,4-d]pyrimidines. J. Med. Chem. *40*, 3601–3616.
19. Traxler, P.M., Furet, P., Mett, H., Buchdunger, E., Meyer, T., and Lydon, N. (1996). 4-(Phenylamino)pyrrolopyrimidines: potent and selective, ATP site directed inhibitors of the EGF-receptor protein tyrosine kinase. J. Med. Chem. *39*, 2285–2292.
20. Zimmermann, J., Buchdunger, E., Mett, H., Meyer, T., and Lydon, N.B. (1997). Potent and selective inhibitors of the ABL-kinase: phenylaminopyrimidine (PAP) derivatives. Bioorg. Med. Chem. Lett. *7*, 187–192.
21. Fong, T.A.T., Shawver, L.K., Sun, L., Tang, C., App, H., Powell, T.J., Kim, Y.H., Schreck, R., Wang, X., Risau, W., et al. (1999). SU5416 is a potent and selective inhibitor of the vascular endothelial growth factor receptor (Flk-1/KDR) that inhibits tyrosine kinase catalysis, tumor vascularization, and growth of multiple tumor types. Cancer Res. *59*, 99–106.
22. Sun, L., Tran, F., App, H., Hirth, P., McMahon, G., and Tang, C. (1998). Synthesis and biological evaluations of 3-substituted indolin-2-ones: a novel class of tyrosine kinase inhibitors that exhibit selectivity toward particular receptor tyrosine kinases. J. Med. Chem. *41*, 2588–2603.
23. Vesely, J., Havlicek, L., Strnad, M., Blow, J.J., Donella-Deana, A., Pinna, L., Letham, D.S., Kato, J.Y., Detivaud, L., Leclerc, S., et al. (1994). Inhibition of cyclin-dependent kinases by purine analogs. Eur. J. Biochem. *224*, 771–786.

24. De Azevedo, W.F., Leclerc, S., Meijer, L., Havlicek, L., Strnad, M., and Kim, S.H. (1997). Inhibition of cyclin-dependent kinases by purine analogs. Crystal structure of human cdk2 complexed with roscovitine. Eur. J. Biochem. *243*, 518–526.
25. Gray, N.S., Wodicka, L., Thunnissen, A.-M.W.H., Normann, T.C., Kwon, S., Espinoza, F.H., Morgan, D.O., Barnes, G., LeClerc, S., Meijer, L., et al. (1998). Exploiting chemical libraries, structure, and genomics in the search for kinase inhibitors. Science *281*, 533–538.
26. Knockaert, M., Greengard, P., and Meijer, L. (2002). Pharmacological inhibitors of cyclin-dependent kinases. Trends Pharmacol. Sci. *23*, 417–425.
27. Chang, Y.T., Gray, N.S., Rosania, G.R., Sutherlin, D.P., Kwon, S., Norman, T.C., Sarohia, R., Leost, M., Meijer, L., and Schultz, P.G. (1996). Synthesis and application of functionally diverse 2,6,9-trisubstituted purine libraries as CDK inhibitors. Chem. Biol. *5*, 361–375.
28. Legraverend, M., Tunnah, P., Noble, M., Ducrot, P., Ludwig, O., Grierson, D.S., Leost, M., Meijer, L., and Endicott, J. (2000). Cyclin-dependent kinase inhibition by new C-2 alkynylated purine derivatives and molecular structure of a CDK2-inhibitor complex. J. Med. Chem. *43*, 1282–1292.
29. Lee, J.C., Badger, A.M., Griswold, D.E., Dunnington, D., Truneh, A., Votta, B., White, J.R., Young, P.R., and Bender, P.E. (1993). Bicyclic imidazoles as a novel class of cytokine biosynthesis inhibitors. Ann. N Y Acad. Sci. *696*, 149–170.
30. Adams, J.L., Boehm, J.C., Kassis, S., Gorycki, P.D., Webb, E.F., Hall, R., Sorenson, M., Lee, J.C., Ayrton, A., Grisword, D.E., et al. (1998). Pyrimidinylimidazole inhibitors of CSBP/p38 kinase demonstrating decreased inhibition of hepatic cytochrome P450 enzymes. Bioorg. Med. Chem. Lett. *8*, 3111–3116.
31. Laufer, S.A., Wagner, G.K., Kotschenreuther, D.A., and Albrecht, W. (2003). Novel substituted pyridinyl imidazoles as potent anticytokine agents with low activity against hepatic cytochrome P450 enzymes. J. Med. Chem. *46*, 3230–3244.
32. Carlson, B.A., Dubay, M.M., Sausville, E.A., Brizuela, L., and Worland, P.J. (1996). Flavopiridol induces G1 arrest with inhibition of cyclin-dependent kinase (CDK) 2 and CDK4 in human breast carcinoma cells. Cancer Res. *56*, 2973–2978.
33. Losiewicz, M.D., Carlson, B.A., Kaur, G., Sausville, E.A., and Worland, P.J. (1994). Potent inhibition of Cdc2 kinase activity by the flavonoid L86–8275. Biochem. Biophys. Res. Commun. *201*, 589–595.
34. Zaharevitz, D.W., Gussio, R., Leost, M., Senderowicz, A.M., Lahusen, T., Kunick, C., Meijer, L., and Sausville, E.A. (1999). Discovery and initial characterization of the paullones, a novel class of small-molecule inhibitors of cyclin-dependent kinases. Cancer Res. *59*, 2566–2569.
35. Schultz, C., Link, A., Leost, M., Zaharevitz, D.W., Gussio, R., Sausville, E.A., Meijer, L., and Kunick, C. (1999). Paullones, a series of cyclin-dependent kinase inhibitors: synthesis, evaluation of CDK1/cyclin B inhibition, and *in vitro* antitumor activity. J. Med. Chem. *42*, 2909–2919.
36. Leost, M., Schultz, C., Link, A., Wu, Y.-Z., Biernat, J., Mandelkow, E.-M., Bibb, J.A., Snyder, G.L., Greengard, P., Zaharevitz, D.W., et al. (2000). Paullones are potent inhibitors of glycogen synthase kinase-3b and cyclin-dependent kinase 5/p25. Eur. J. Biochem. *267*, 5983–5994.
37. Furusaki, A., Hashiba, N., Matsumoto, T., Hirano, A., Iwai, Y., and Omurs, S. (1982). The crystal and molecular structure of staurosporine, a new alkaloid from a Streptomyces strain. Bull. Chem. Soc. Jpn. *55*, 3681–3685.
38. Gadbois, D.M., Hamaguchi, J.R., Swank, R.A., and Bradbury, E.M. (1992). Staurosporine is a potent inhibitor of p34cdc2 and p34cdc2-like kinases. Biochem. Biophys. Res. Commun. *184*, 80–85.
39. Hudkins, R.L., Iqbal, M., Park, C.-H., Goldstein, J., Herman, J., Shek, E., Murakata, C., and Mallamo, J.P. (1998). Prodrug esters of the indolocarbazole CEP-751 (KT-6587). Bioorg. Med. Chem. Lett. *8*, 1873–1876.
40. Cimino, G., De Rosa, S., De Stefano, S., Mazzarella, L., Puliti, R., and Sodano, G. (1982). Isolation and x-ray crystal structure of a novel bromo compound from two marine sponges. Tetrahedron Lett. *23*, 767–768.
41. Kitagawa, I., Kobayashi, M., Kitanaka, K., Kido, M., and Kyogoku, Y. (1983). Marine natural products. XII. On the chemical constituents of the Okinawan marine sponge *Hymeniacidon aldis*. Chem. Pharm. Bull. *31*, 2321–2328.
42. De Nanteuil, G., Ahond, A., Guilhem, J., Poupat, C., Tran Huu Dau, E., Potier, P., Pusset, M., Pusset, J., and Laboute, P. (1985). Marine invertebrates from the New Caledonian lagoon. V. Isolation and identification of metabolites of a new species of sponge, *Pseudaxinyssa cantharella*. Tetrahedron Lett. *41*, 6019–6033.
43. Schmitz, F.J., Gunasekera, S.P., Lakshmi, V., and Tillekeratne, L.M.V. (1985). Marine natural products: pyrrololactams from several sponges. J. Nat. Prod. *48*, 47–53.
44. Pettit, G.R., Herald, C.L., Leet, J.E., Gupta, R., Schaufelberger, D.E., Bates, R.B., Clewlow, P.J., Doubek, D.L., Manfredi, K.P., Rützler, K., et al. (1990). Antineoplastic agents. 168. Isolation and structure of axinohydantoin. Can. J. Chem. *68*, 1621–1624.
45. Meijer, L., Thunnissen, A.-M.W.H., White, A.W., Garnier, M., Nikolic, M., Tsai, L.-H., Walter, J., Cleverley, K.E., Salinas, P.C., Wu, Y.-Z., et al. (1999). Inhibition of cyclin-dependent kinases, GSK-3β and CK1 by hymenialdisine, a marine sponge constituent. Chem. Biol. *7*, 51–63.
46. Tasdemir, D., Mallon, R., Greenstein, M., Feldberg, L.R., Kim, S.C., Collins, K., Wojciechowicz, D., Mangalindan, G.C., Concepción, G.P., Harper, M.K., et al. (2002). Aldisine alkaloids from the Philippine sponge *Stylissa massa* are potent inhibitors of mitogen-activated protein kinase kinase-1 (MEK-1). J. Med. Chem. *45*, 529–532.
47. Curman, D., Cinel, B., Williams, D.E., Rundle, N., Block, W.D., Goodarzi, A.A., Hutchins, J.R., Clarke, P.R., Zhou, B.-B., Lees-Miller, S.P., et al. (2001). Inhibition of the G2 DNA damage checkpoint and of protein kinases Chk1 and Chk2 by the marine sponge alkaloid debromohymenialdisine. J. Biol. Chem. *276*, 17914–17919.
48. Nishizuka, Y. (1988). The molecular heterogeneity of protein kinase C and its implications for cellular regulation. Nature *334*, 661–665.
49. Nishizuka, Y. (1989). The family of protein kinase C for signal transduction. JAMA *262*, 1826–1833.
50. Nambi, P., and Patil, A.D. (September, 1993). Imidazolinylidenepyrroloazepine derivatives as protein kinase C inhibitor. Patent WO-9316703.
51. Breton, J.J., and Chabot-Fletcher, M.C. (1997). The natural product hymenialdisine inhibits interleukin-8 production in U937 cells by inhibition of nuclear factor-κB. J. Pharmacol. Exp. Ther. *282*, 459–466.
52. Roshak, A., Jackson, J.R., Chabot-Fletcher, M., and Marshal, L.A. (1997). Inhibition of NFκB-mediated interleukin-1β-stimulated prostaglandin E_2 formation by the marine natural product hymenialdisine. J. Pharmacol. Exp. Ther. *283*, 955–961.
53. Badger, A.M., Cook, M.N., Swift, B.A., Newman-Tarr, T.M., Gowen, M., and Lark, M. (1999). Inhibition of interleukin-1-induced proteoglycan degradation and nitric oxide production in bovine articular cartilage/chondrocyte cultures by the natural product, hymenialdisine. J. Pharmacol. Exp. Ther. *290*, 587–593.
54. Knockaert, M., Gray, N., Damiens, E., Chang, Y.-T., Grellier, P., Grant, K., Fergusson, D., Mottram, J., Soete, M., Dubremetz, J.-F., et al. (2000). Intracellular targets of cyclin-dependent kinase inhibitors: identification by affinity chromatography using immobilised inhibitors. Chem. Biol. *7*, 411–422.
55. Knockaert, M., Wieking, K., Schmitt, S., Leost, M., Grant, K.M., Mottram, J.C., Kunick, C., and Meijer, L. (2002). Intracellular targets of paullones. Identification following affinity purification on immobilized inhibitor. J. Biol. Chem. *277*, 25493–25501.
56. Annoura, H., and Tatsuoka, T. (1995). Total syntheses of hymenialdisine and debromohymenialdisine: stereospecific construction of the 2-amino-4-oxo-2-imidazolin-5(Z)-disubstituted ylidene ring system. Tetrahedron Lett. *36*, 413–416.
57. Xu, Y.-Z., Yakushijin, K., and Horne, D.A. (1997). Synthesis of C11N5 marine sponge alkaloids: (±)-hymenin, stevensine, hymenialdisine, and debromohymenialdisine. J. Org. Chem. *62*, 456–464.
58. Sosa, A.C.B., Yakushijin, K., and Horne, D.A. (2000). A practical

synthesis of (Z)-debromohymenialdisine. J. Org. Chem. *65*, 610–611.
59. Chacun-Lefévre, L., Joseph, B., and Mérour, J.-Y. (2000). Synthesis and reactivity of azepino[3,4-b]indol-5-yl trifluoromethanesulfonate. Tetrahedron *56*, 4491–4499.
60. Chacun-Lefévre, L., Joseph, B., and Mérour, J.-Y. (2001). Intramolecular Heck coupling of alkenyl 3-iodoindole-2-carboxamide derivatives. Synlett. *6*, 848–850.
61. Erdélyl, M., and Gogoll, A. (2001). Rapid homogeneous-phase Sonogashira coupling reactions using controlled microwave heating. J. Org. Chem. *66*, 4165–4169.
62. Kearns, A.E., Donohue, M.M., Sanyal, B., and Demay, M.B. (2001). Cloning and characterization of a novel protein kinase that impairs osteoblast differentiation *in vitro*. J. Biol. Chem. *276*, 42213–42218.
63. Primot, A., Baratte, B., Gompel, M., Borgne, A., Liabeuf, S., Romette, J.-L., Jho, E.-h., Costantini, F., and Meijer, L. (2000). Purification of GSK-3 by affinity chromatography on immobilized axin. Protein Expr. Purif. *20*, 394–404.
64. Davis, S.P., Reddy, H., Caivano, M., and Cohen, P. (2000). Specificity and mechanism of action of some commonly used protein kinase inhibitors. Biochem. J. *251*, 95–105.
65. Bain, J., McLauchan, H., Elliott, M., and Cohen, P. (2003). The specificities of protein kinase inhibitors: an update. Biochem. J. *371*, 199–204.
66. Cho, H., and Matsuki, S. (1996). Ring construction of several heterocycles with phosphorus pentoxide-methanesulfonic acid (PPMA). Heterocycles *43*, 127–131.
67. Kano, S., Yokomatsu, T., Nemoto, H., and Shibuya, S. (1985). An efficient diastereoselective synthesis of 6-hydroxy-4a-[3,4-crowned(15-crown-5)phenyl]-trans-decahydroisoquinoline. Tetrahedron Lett. *26*, 1531–1534.
68. Kano, S., Yokomatsu, T., Nemoto, H., and Shibuya, S. (1986). Effect of A-strain on a diastereoselective synthesis of 6-hydroxy-4a-aryldecahydroisoquinolines; revised structures of N-acyliminium ion-polyene cyclization products. J. Org. Chem. *51*, 561–564.
69. Jones, G., Willett, P., Glen, R.C., Leach, A.R., and Taylor, R. (1997). Development and validation of a genetic algorithm for flexible docking. J. Mol. Biol. *267*, 727–748.
70. Tarricone, C., Dhavan, R., Peng, J., Areces, L.B., Tsai, L.H., and Musacchio, A. (2001). Structure and regulation of the CDK5-p25 (nck5a) complex. Mol. Cell *8*, 657–669.
71. Davies, T.G., Tunnah, P., Meijer, L., Marko, D., Eisenbrand, G., Endicott, J.A., and Noble, M.E. (2001). Inhibitor binding to active and inactive CDK2: the crystal structure of CDK2-cyclin A/indirubin-5-sulphonate. Structure *9*, 389–397.
72. Shevchenko, A., Wilm, M., Vorm, O., and Mann, M. (1996). Mass spectrometric sequencing of proteins silver-stained polyacrylamide gels. Anal. Chem. *68*, 850–858.
73. Kussmann, M., Nordhoff, E., Rahbek-Nielsen, H., Haebel, S., Rossel-Larsen, M., Jakobsen, L., Gobom, J., Mirgorodskaya, E., Kroll-Kristensen, A., Palm, L., et al. (1997). Matrix-assisted laser desorption/ionization mass spectrometry sample preparation techniques designed for various peptide and protein analytes. J. Mass Spectrom. *32*, 593–601.
74. Zhang, W., and Chait, B.T. (2000). ProFound: an expert system for protein identification using mass spectrometric peptide mapping information. Anal. Chem. *72*, 2482–2489.
75. Cook, N.D. (1996). Scintillation proximity assay—a versatile high throughput screening technology. Drug Discov. Today *1*, 287–294.